

# Wide Field Surveys of Herbig-Haro Objects

Jun Yan<sup>1,2</sup>, Hongchi Wang<sup>1,2</sup>, Min Wang<sup>1,2</sup>, Licai Deng<sup>1</sup>, Ji Yang<sup>2</sup> & Jiansheng Chen<sup>1</sup>

<sup>1</sup>Beijing Astronomical Observatory, Academia Sinica, Beijing 100080, PR China

<sup>2</sup>Purple Mountain Observatory, Academia Sinica, Nanjing 210008, PR China

## ABSTRACT

We report our new results from wide-field surveys of Herbig-Haro (HH) objects in the nearby star forming regions. The surveys covered approximately  $56 \text{ deg}^2$  in Perseus, Taurus, Orion, Monoceros, and other regions. Using refined techniques, we discovered in total 68 HH objects, of which 32 were in Perseus, 4 in Taurus, 13 in Orion, 18 in Monoceros, and 1 in S287 regions. The newly discovered HH objects demonstrate a great variety of morphological structures, including 5 jets, 7 arcs, 12 cirri or cirrus groups, 13 patches, and many knots. These objects provide a new comprehensive database for the study of HH objects in the regions of recent star formation.

## 1. Introduction

Herbig-Haro (HH) objects are small shock-excited nebulae intimately associated with star forming regions (see reviews by Schwartz 1983 and Raga 1989). Like high velocity CO molecular outflows and shock-excited near-IR emissions of  $\text{H}_2$ , HH objects are good tracers of the mass outflow activities of young stellar objects (YSOs) and can be used to trace the extremely young class 0 objects embedded in dense molecular cores – about 30% class 0 objects are now known to be associated with HH objects (Eiroa et al 1994).

The prototype HH objects, HH 1 and 2, were discovered by Herbig (1951) and Haro (1952) in their  $\text{H}_\alpha$  emission star survey. Since then about 300 HH objects have been found by several searching methods, including objective-prism Schmidt survey, narrow-band CCD imaging, near-IR imaging, and other methods (Reipurth 1994).

In this paper, we describe the way of our large-field CCD Schmidt surveys of HH objects using intermediate band filters, and report the discovery of a large number of new HH objects in Perseus, Taurus, Orion, Monoceros, and other star forming regions.

## 2. Observations and Identification Techniques

### 2.1. Instrumentation and Filters

The observations of the surveys were carried out at Xinglong Station of Beijing Astronomical Observatory (BAO) during the winters of 1995-1997. The telescope used is the BAO  $f/3 \text{ 60/90cm}$

Schmidt telescope equipped with a 2k×2k Aerospace Ford CCD which has a pixel size of  $15\mu$ , corresponding to a resolution of  $1.67''/\text{pixel}$ , and has a total field of view of  $58'$ . On average, the seeing at the site is around  $2''$ . The filter set used in this program are two BATC<sup>1</sup> intermediate band filters [BATC09], [BATC10], and a narrow band filter [BATC26]. The parameters of the filters are given in Table 1. As shown in this table, the [BATC09] filter well covers the strong and characteristic lines of HH objects, while the [BATC10] band has no strong lines of these objects and, therefore, can be used to represent the continuum.

Table 1: Filter Parameters

Filter ID	Central Wavelength	Band Width	Property
[BATC09]	$6660\text{\AA}$	$480\text{\AA}$	[NII], $H_\alpha$ , [SII]
[BATC10]	$7050\text{\AA}$	$300\text{\AA}$	Continuum
[BATC26]	$6725\text{\AA}$	$50\text{\AA}$	[SII] $\lambda\lambda 6717/6731$

## 2.2. Field Selection

HH objects are produced by interactions of mass outflows of YSOs with the surrounding medium (Schwartz 1975). They are associated with other tracers of the activities of YSOs, such as molecular outflows,  $H_2O$  or OH masers, and they usually occurs in groups. For the purpose of large field surveys of HH objects in star forming regions, we have selected 56 fields in the surveys based on the following selection criteria:

1. There are known HH objects, molecular outflows,  $H_2O$  or OH masers in or near the field;
2. There are IRAS sources of class 0 or class 1, VLA continuum emissions in the field;
3. There are GGD or RNO objects in the field.

Table 2 gives the log of the surveys.

## 2.3. Identification Techniques

Our survey sequence includes a first-step quick survey for HH candidates (Runs A and B in Table 2 ) and a narrow-band identification (Runs C and D). The subsequent observations of this survey program is in progress, and the details of each target field will be reported in a later paper

---

<sup>1</sup>BATC-Beijing-Arizona-Taiwan-Connetticut Multicolor Sky Survey

Table 2: Log of observations

Field id	Field Center (1950)		Exposure Time and Date				Run*
	R.A.	DEC	[BATC09](min.)	[BATC10](min.)	Run*	[BATC26](min.)	
A01	03:21:30	30:10:00	15	15	A		
A02	03:25:30	30:10:00	15	15	A	60	C
A03	03:29:30	30:10:00	15	15	A	60	C
A04	03:21:30	31:00:00	15	15	A		
A05	03:25:30	31:00:00	15	15	A	60	C
A06	03:29:30	31:00:00	15	15	A	60	C
A07	03:41:20	31:25:00	15	15	A		
A08	03:45:20	31:25:00	20	18	A		
A09	03:41:20	32:15:00	15	15	A		
A10	03:45:20	32:15:00	15	15	A	60	C
A11	04:24:27	26:00:00	20	20	A		
A12	04:31:17	22:50:00	24	24	A	60	C
A13	04:01:41	26:00:00	24	24	A		
A14	04:35:20	25:18:00	15	20	A		
A15	04:32:00	24:18:00	15	15	A		
A16	04:28:00	24:18:00	15	15	A		
A17	04:15:20	28:00:00	15	15	A		
A18	04:17:00	27:03:00	15	15	A		
A19	04:19:04	19:25:00	15	15	A		
B01	05:48:40	01:55:00	20	20	B		
B02	05:48:40	02:50:00	20	20	B	60	C
B03	05:52:20	01:55:00	20	20	B		
B04	05:52:20	02:50:00	20	20	B	60	D
B05	06:06:00	-06:20:00	24	24	B	60	C
B06	06:09:40	-06:20:00	24	24	B		
B07	04:27:17	22:50:00	24	24	B		
B08	04:35:17	22:50:00	24	24	B		
B09	06:57:30	-04:35:00	24	24	B	60	D
B10	06:57:17	-07:42:16	6	24	B		
B11	03:33:20	30:35:00	20	20	B		
B12	07:02:45	-11:15:00	20	20	B		
B13	06:38:20	10:35:00	20	20	B	60	D
B14	03:33:20	31:25:00	20	20	B		
B15	03:37:20	30:35:00	20	20	B		
B16	06:38:20	09:40:00	20	20	B	60	D
B17	06:05:46	21:35:00	20	20	B		
B18	03:37:20	31:25:00	20	20	B		
B19	03:37:20	32:15:00	20	20	B		
B20	03:41:20	30:35:00	20	20	B		
B21	06:06:00	18:00:00	20	20	B		
B22	06:09:50	18:00:00	20	20	B		
B23	03:03:32	58:19:00	20	20	B		
B24	03:23:00	58:36:00	20	20	B		
B25	06:11:48	13:51:00	20	20	B	60	D
B26	03:45:20	33:05:00	20	20	B		
B27	06:56:46	-03:53:00	20	20	B		
B28	06:45:20	-02:09:30	20	20	B		
B29	06:36:30	08:50:00	20	20	B		
B30	06:31:00	04:10:00	20	20	B		
B31	05:59:00	16:15:00	20	20	B		
B32	05:36:00	35:55:00	20	20	B		
B33	05:34:30	31:58:00	20	20	B		
B34	05:44:00	-00:50:00	30	20	B		
B35	05:44:00	00:04:00	20	20	B	60	D
B36	05:44:00	00:58:00	20	20	B		
B37	05:40:20	-01:44:00	20	20	B	60	D

(\*) Run code: A-Oct 15,1995~Dec 20,1995; B-Feb 13,1996~Mar 18,1996;  
 C-Dec 6,1996~Dec 9,1996; D-Mar 7,1997~Mar 11,1997

(Yan et al. 1997). Here we give the techniques of picking up new HH objects and some snapshots of our first results. For a target field, 3 or more frames in both [BATC09] and [BATC10] bands were taken and combined so that the cosmic rays and the bad pixels were eliminated in the resultant images. The two resultant frames in [BATC09] and [BATC10] bands were blinked and compared. Due to their strong emissions in  $H_\alpha$ , [NII] and [SII] lines, HH objects are prominent in [BATC09] band but usually invisible in [BATC10] band because of their very low continuum emission in this passband. HH candidates were picked up from the careful comparison between the two images. The minimum angular size of detectable candidates is limited by the pixel size and is about  $2''$  in our surveys. In this step we picked up about 150 HH candidates in the 56 fields.

In the first step there is some possibility of contamination by compact HII regions and reflection nebulae. Our second step is to identify the candidates using the narrow-band [BATC26] filter, which covers two characteristic lines of HH object,  $\lambda\lambda 6717, 6731$ . We have made this further identification in 15 fields out of the 56 target fields in table 2. Three frames, each with an exposure time of 20 minutes, were taken; Then the frames were reduced just as in the [BATC09] and [BATC10] bands. We found that above 90 percent of the candidates of HH objects from our first step are identifiable in the [BATC26] band. The images of HH objects are sharper in the [BATC26] frames than in the [BATC09] frames. In contrast, the compact HII regions and reflection nebulae are invisible in the [BATC26] frames.

In order to demonstrate the effectiveness of our surveys, we present in Figure 1 four sample fields out of the long list of Table 3. For each field, we give 3 images taken with our filter set in a row of the image array of Figure 1. The first column is the narrow band [BATC26] images, the second and third columns are [BATC10] and [BATC09] band images, respectively. The HH objects detected in both [BATC26] and [BATC09] bands are markeded using the numbers assigned in our surveys. In all the fields, HH objects show up only in [BATC09] and [BATC26] bands, with their images more prominent in [BATC26], whereas they are completely invisible in [BATC09] band. The first field, labeled *A02* in the top row, has dimensions of  $512 \times 512$  pixels, in which the HH objects 1A, 1B, 1C and 4, 5 are coincident, respectively, with HH279C, HH279B, HH279A and HH317, HH318 in Bally et al.’s list (Bally et al. 1996, 1997), therefore this field may also serve as a comparison of our observations with theirs. Comparing with their work, it is clear that all the HH objects falling into the region overlaped with Bally et al.’s (1997) were picked up using our method. The rest rows are 3 other HH object survey fields: A06, A10, and A12, whose sizes are, respectively,  $200 \times 200$ ,  $300 \times 300$  and  $200 \times 200$  in pixels. A02 is located in L1455, A12 is in the vicinity of CI Tau, and A06 is located at about  $1^\circ$  east of NGC1333.

### 3. Results and Discussion

From the 56 target fields, we discovered more than 150 HH candidates by comparison between [BATC09] and [BATC10] frames. From the 15 [BATC26] fields, we identified 68 new HH objects. These objects are listed in Table 3. In the table, column 1 is the numbers of the newly detected

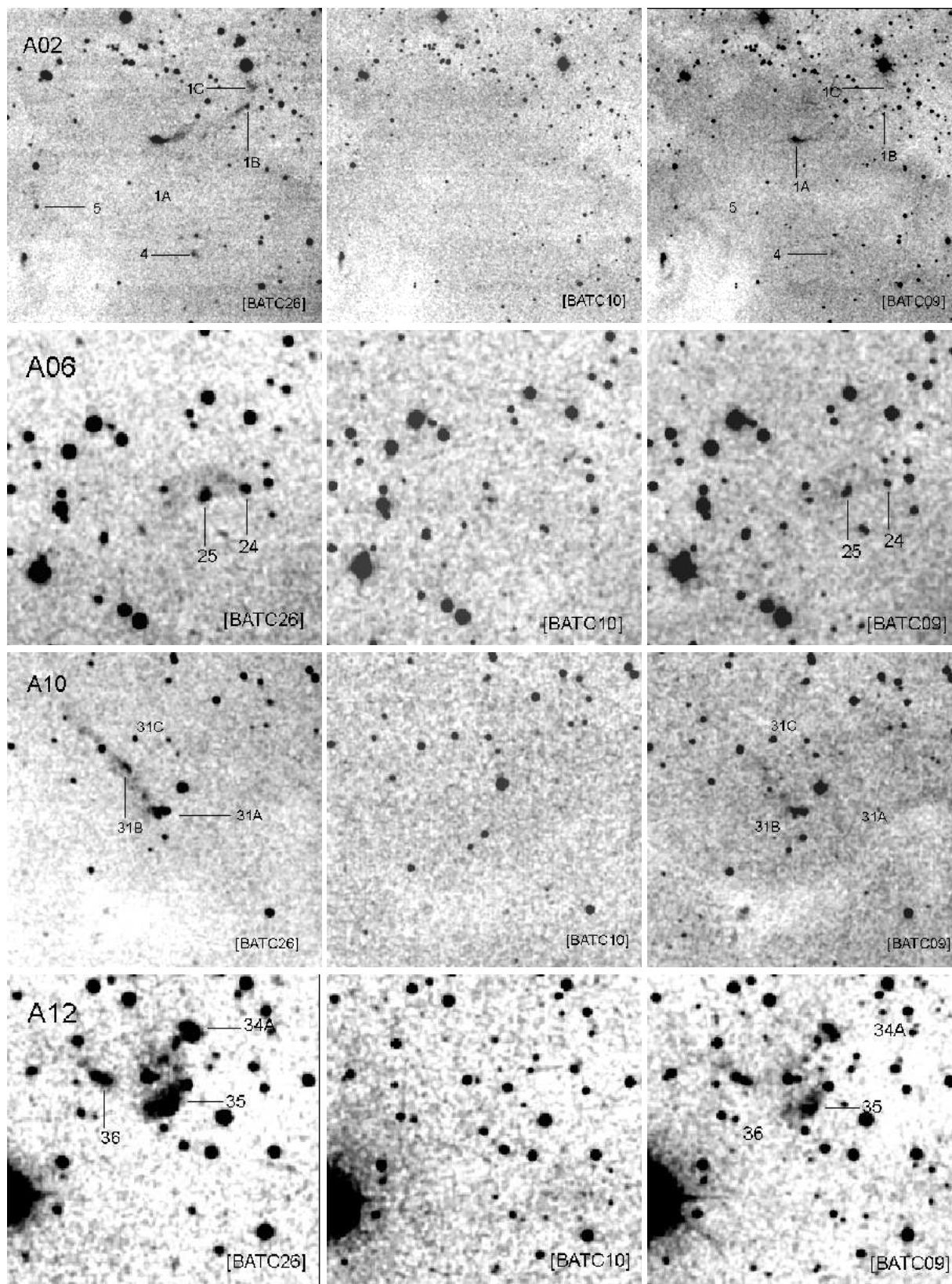


Fig. 1.— The [BATC26], [BATC10], and [BATC09] band images of 4 sample fields of our surveys, each row corresponds to a field. For details see text.

HH objects assigned in our surveys, columns 2 and 3 are, respectively, the right ascension and declination in 1950 epoch. The source positions were derived using the Guide Star Catalog. The overall accuracy is estimated to be about 0.5 arcsec (Fan et al. 1996). A brief comment to each object is given in column 4. Among the 68 objects, 15 objects coincide with those reported by Bally, Devine, & Reipurth (1996) and Bally et al. (1997). These objects are all in the fields A02 and A05, which are the central part of NGC 1333 in Perseus.

According to their morphological properties, the new HH objects are classified into knots, jets, arcs, patches, and cirri. Most of the 68 new HH objects are either bright or faint knots, while a few of them are cirri or cirrus groups, arcs, and jets. There are 7 HH objects showing arc structures, including No.1A, 7, 8, 11, 60, 62 and 63. Objects No.1, 9, 31, 34, and 56 are remarkable in that they show extended jets. HH No.1A, which is coincident with HH 279C in Bally et al. (1997), extends to No.1C (HH279A in Bally et al. 1997) forming a large jet structure, as clearly shown in the top row of Fig 1. HH objects No.31A and 31B are two main knots of a spectacular jet in the field A10, which is located at about  $2^\circ$  east of Barnard 5. It is also possible that the jet-like HH flows of HH No.31A, 31B, and 31C are the northern part of a bow structure with the apex at HH No.31A. We note that about one third of the newly discovered HH objects occur in groups. By the term “occur in group” we mean that in the vicinity of 0.5 pc from a HH object there is at least one other HH object.

For the local star forming regions, where the fields are rarely contaminated by the compact HII regions, We believe that the filter combination of [BATC09] and [BATC10] is an efficient and reliable procedure to find new HH objects.

We specially thank the staff of BATC Beijing group for observation time allocation, for their helpful discussion, for their hospitality and excellent support. This research is supported in part by NSFC grant 19673020.

## REFERENCES

- Bally, J. & Devine, D., 1996, ApJ, 473, L49  
Bally, J., Devine, D., Alten, V. & Sutherland, R. S., ApJ, 478, 603  
Eiroa, C., Miranda, L., Anglada, G., Estellella, R. & Torrelles, J, 1994, A&A, 283, 973  
Fan, X. et al. 1996, AJ, 112, 628  
Haro, G., 1952, ApJ, 115, 572  
Herbig, G. H., 1951, ApJ, 113, 197  
Raga, A.C., 1989, in ESO Workshop on *Low Mass Star Formation and Pre-Main Sequence Objects*, ed. B. Reipurth (Garching:ESO), 281

Reipurth, B., 1994, A General Catalog of Herbig-Haro Objects  
(<ftp://ftp.hq.eso.org/pub/Catalogs/Herbig-Haro>)

Schwartz, R. D., 1975, ApJ, 195, 631

Schwartz, R. D., 1983, ARA&A, 21, 209

Yan, J., Wang, H.C., Wang, M., Deng, L., Yang, J. & Chen, J.S., 1997, *in preparation for AJ*

Table 3: A List of New Herbig-Haro Objects

PMO No	RA. (1950)	DEC. (1950)	Comments
1A	3:24:14.56	30:06:50.5	arc (HH279C)*
1B	3:23:54.97	30:08:13.7	jet (HH279B)*
1C	3:23:53.59	30:09:09.4	cirrus (HH279A)*
2	3:23:55.03	31:25:41.2	bright knot with star
3	3:23:55.42	30:15:31.1	knot (HH278)*
4	3:24:07.40	30:01:29.1	cirrus (HH317)*
5	3:24:40.65	30:03:53.3	knot (HH318)*
6A	3:25:07.45	31:09:21.8	knot (HH338A)*
6B	3:25:06.12	31:07:52.6	cirrus (HH338C)*
7	3:25:10.03	30:39:36.3	arc (HH351)*
8	3:25:44.91	30:59:17.6	arc (HH341)*
9A	3:25:48.99	30:55:02.2	knot (HH343A)*
9B	3:25:46.55	30:55:23.5	jet (HH343D)*
10	3:25:49.30	30:42:06.9	two knots
11	3:25:49.44	30:54:24.0	arc (HH350)*
12A	3:25:55.40	31:02:55.9	knot (HH344A)*
12B	3:25:53.98	31:01:57.1	knot (HH344B)*
13A	3:26:10.15	31:05:04.9	knot (HH347B)*
13B	3:26:11.59	31:05:07.4	knot (HH347A)*
14	3:26:12.64	30:49:33.6	knot (HH352)*
15	3:26:21.76	31:03:16.6	cirrus (HH348)*
16A	3:26:32.79	31:20:02.5	patch (HH353)*
16B	3:26:28.14	31:19:56.1	cirrus
17	3:26:30.68	31:03:17.2	cirrus (HH349)*
18	3:27:28.59	30:17:36.7	comma-like knot
19	3:27:33.11	30:11:43.4	knot
20	3:27:40.89	30:19:11.1	knot
21	3:27:42.39	30:27:50.9	knot
22	3:27:48.56	30:14:28.1	faint patch
23A	3:27:52.26	30:24:40.0	faint patch
23B	3:27:55.29	30:25:07.6	faint patch
24	3:28:42.35	30:59:50.3	bright knot
25	3:28:45.84	30:59:43.5	bright knot
26	3:29:21.71	31:14:31.8	faint patch
27	3:29:58.81	31:16:12.7	bright knot with faint cirrus
28	3:30:09.16	30:59:03.5	knot
29A	3:30:27.49	30:59:40.8	knot
29B	3:30:29.77	30:58:47.3	group of knots
30A	3:30:43.72	30:54:54.5	knot with cirrus
30B	3:30:44.37	30:54:58.3	knot
30C	3:30:44.48	30:55:01.3	knot
30D	3:30:45.03	30:55:20.1	knot
31A	3:43:49.77	32:36:03.8	bright knot,SE part of the jet
31B	3:43:53.81	32:37:06.9	knot,middle part of the jet
31C	3:43:58.57	32:37:58.8	patch,NW part of the jet
32	3:43:56.54	32:33:47.2	several faint knots
33	4:30:12.46	22:48:51.8	knot
34A	4:31:12.99	23:03:16.2	bright knot
34B	4:31:14.22	23:03:09.4	knot,middle part of jet
34C	4:31:15.26	23:02:47.1	knot,middle part of jet
35	4:31:14.90	23:01:55.7	bright knot



Table 3: -Continued

No	RA. (1950)	DEC. (1950)	Comments
36	4:31:20.15	23:02:28.0	bright knot
37A	5:39:14.36	-1:46:28.1	bright knot
37B	5:39:11.50	-1:47:52.8	bright knot
38	5:44:02.11	0:24:59.0	knot with cirrus
39	5:44:07.94	0:24:34.2	knot
40	5:44:31.73	0:20:45.7	bright knot
41A	5:44:33.49	0:10:45.5	knot
41B	5:44:36.90	0:09:58.4	knot
41C	5:44:38.39	0:09:59.5	knot
42	5:44:33.96	0:23:51.8	faint knot
43A	5:45:33.12	0:17:58.3	knot
43B	5:45:30.00	0:18:14.7	diffuse faint patch
44A	5:45:45.02	0:24:46.3	knot
44B	5:45:44.13	0:24:39.4	faint knot
45	5:47:25.85	2:52:14.9	2' diameter complex
46	5:48:31.27	2:41:06.9	knot
47	5:49:26.63	3:01:33.0	knot
48	5:50:55.10	2:40:58.7	knot
49	5:51:33.01	2:36:37.7	knot
50A	6:04:27.85	-5:53:02.0	faint knot
50B	6:04:27.28	-5:54:05.1	faint knot
51A	6:13:03.15	14:18:51.8	bright arc-like knot
51B	6:13:05.50	14:18:22.7	knot
51C	6:13:07.32	14:17:25.6	knot
51D	6:13:07.91	14:17:56.3	knot
52A	6:37:02.24	10:08:50.9	knot
52B	6:37:00.58	10:09:21.6	curved chain
52C	6:36:53.47	10:09:38.7	cirrus
52D	6:36:50.59	10:10:01.6	cirrus
53	6:37:33.83	10:21:36.2	bright complex
54	6:37:45.51	9:56:16.5	knot with diffuse patches
55	6:37:46.25	10:10:47.0	knot
56	6:37:48.39	10:12:46.5	chained knots or jet
57A	6:37:50.44	10:42:42.3	bright knot
57B	6:38:02.18	10:41:26.3	bright patch
57C	6:38:13.99	10:38:53.9	patch
57D	6:38:24.57	10:38:39.7	patch
57E	6:38:37.43	10:42:27.9	knot with cirrus
58A	6:37:54.97	10:14:57.6	knot alined with 58B,58C
58B	6:37:55.64	10:15:17.2	knot
58C	6:37:55.85	10:15:36.5	knot
59	6:37:59.95	9:35:42.4	knot
60	6:38:01.08	10:08:10.4	arc
61A	6:38:09.89	10:09:34.1	bright knot
61B	6:38:08.54	10:09:11.7	bright knot
62	6:38:13.75	10:16:41.1	5' bright arc
63	6:38:13.76	9:35:48.8	arc
64A	6:38:27.30	9:32:16.1	bright patch
64B	6:38:31.04	9:32:03.1	bright patch
65	6:38:37.15	9:33:34.2	bright patch
66	6:38:38.54	9:30:55.5	bright knot
67	6:38:42.36	10:26:41.3	1' diameter complex
68	6:57:11.21	-4:46:54.2	two knots

(\*) Detected also by Bally, et al. (1996, 1997)